

Transesterification-Induced Cocrystallization of Poly(trimethylene terephthalate) and Poly(butylene succinate) Blends

Yulan Huang,¹ Le Bao,¹ Yiwang Chen,^{1,2} Weihua Zhou,¹ Licheng Tan,^{1,2} Shuaishuai Yuan²

¹*Institute of Polymers/Institute for Advanced Study, Nanchang University, 999 Xuefu Avenue, Nanchang 330031, China*

²*Department of Chemistry, Nanchang University, 999 Xuefu Avenue, Nanchang 330031, China*

Received 17 February 2010; accepted 1 August 2010

DOI 10.1002/app.33122

Published online 23 November 2010 in Wiley Online Library (wileyonlinelibrary.com).

ABSTRACT: A series of copolyesters were prepared by the direct melt transesterification of poly(trimethylene terephthalate) (PTT) and poly(butylene succinate) (PBS). The sequential structure of the copolyesters was analyzed with proton nuclear magnetic resonance spectroscopy, and the randomness of the copolyesters was calculated to be approximately 0.8. The cocrystallization, thermal behavior, and spherulitic morphology were investigated. The melting points of the copolyesters showed a pseudo-eutectic behavior exhibiting isodimorphic cocrystallization. Wide-angle X-ray diffraction indicated that the copolyesters crystallized in PTT crystals when the butylene succinate

(BS) unit content was less than 60% and in the PBS crystals when the BS unit content was greater than 70%. The mechanical properties of the copolyesters were greatly influenced by the sequence lengths of the aromatic and aliphatic units. The incorporation of BS units into the PTT structure led to a faster rate of degradation of the copolyesters because of the decrease in the aromatic sequence length and the increase in the aliphatic sequence length. © 2010 Wiley Periodicals, Inc. *J Appl Polym Sci* 120: 1297–1306, 2011

Key words: crystallization; polyesters; reactive processing

INTRODUCTION

Aromatic–aliphatic copolyesters have been commercialized for many years and are known for their higher thermal stability and mechanical strength as well as lower cost in contrast to aliphatic biodegradable polyesters.¹ The well-known Ecoflex product produced by BASF Co. is a random copolyester of poly(butylene adipate-*co*-terephthalate) with an approximately 1:1 molar ratio of aliphatic units to aromatic units.² Extensive studies focusing on the synthesis, structure analysis, crystallization behavior,

crystal structure, and physical properties of such aromatic–aliphatic copolyesters have been performed.^{3–7}

Generally, a variety of random copolymers are synthesized by melt polycondensation through the mixing of terephthalic acid or terephthalate and several aliphatic diacids with different diols.^{8,9} Furthermore, the reactive blending of already existing homopolymers has been proven to be a successful and inexpensive tool for producing new aromatic–aliphatic copolyesters with intermediate properties.^{10,11} The copolyesters prepared by this technique include poly(1,4-butylene succinate)/poly(1,4-butylene terephthalate), poly(1,4-butylene adipate-*co*-succinate)/poly(1,4-butylene terephthalate), poly(1,4-butylene succinate)/poly(ethylene terephthalate), and poly(butylene terephthalate/succinate/adipate) copolyesters.^{12–15}

Poly(trimethylene terephthalate) (PTT) is a new commercial engineering plastic exhibiting good tensile behavior, resilience, outstanding elastic recovery, and an ability to be colored with different dyes.^{16,17} These characteristics make PTT highly suitable for use in engineering thermoplastic applications as fibers and films.¹⁸ Poly(butylene succinate) (PBS) is one of the most promising biodegradable polyesters because it has mechanical properties similar to those of polyethylene. This polymer shows sufficient

Correspondence to: Y. Chen (ywchen@ncu.edu.cn) or W. Zhou (dramzwh@126.com).

Contract grant sponsor: Natural Science Foundation of Jiangxi Province; contract grant number: 2009GQH0068.

Contract grant sponsor: Jiangxi Provincial Department of Education.

Contract grant sponsor: Program for Innovative Research Team in University of Jiangxi Province.

Contract grant sponsor: Program for New Century Excellent Talents in University; contract grant number: NCET-06-0574.

Contract grant sponsor: Program for Changjiang Scholars and Innovative Research Team in University; contract grant number: IRT0730.

tensile properties and stability against thermal degradation; however, the high cost and relatively slow biodegradation rate due to the high degree of crystallinity limit its further application.^{19,20} To solve these problems, Papageorgiou and Bikiaris²¹ copolymerized a propylene succinate unit with a butylene succinate (BS) unit to prepare copolyesters with a high degradation rate. They also copolymerized trimethylene terephthalate (TT) units with propylene succinate units to afford thermally stable copolyesters with a high enzymatic degradation rate.²²

For copolyesters, higher degradation rates can be achieved with respect to those of the homopolymers, and this is attributable to the limited crystallinity.²³ In most copolymers in which both components are able to crystallize, the degree of crystallinity tends to decrease as the minor component content increases because of the incompatibility between the two components.²⁴ If two crystallizable components of the copolymers can coexist in their crystal lattices, the thermal and mechanical properties of the copolymers can be controlled without a significant loss of crystalline properties.²⁵ Thus, cocrystallization, including isomorphism and isodimorphism, takes place. The former may occur if the two components have similar chemical structures, whereas the latter usually occurs if the two components have dissimilar chemical structures.^{26,27} For example, isomorphism is rarely observed except for poly(hexamethylene naphthalate-*co*-1,4-cyclohexylene naphthalate)⁹ and poly(propylene terephthalate-*co*-succinate) copolymers.²² Isodimorphism is observed in most cases, such as poly(octamethylene terephthalate-*co*-2,6-naphthalate)²⁸ and poly(butylene-*co*-propylene succinate) copolymers.²¹ Various models such as the Flory, Sanchez-Eby, Baur, and Wendling-Suter models have been proposed to describe the thermodynamic cocrystallization of these copolymers.²⁹⁻³²

In our previous study,³³ we successfully synthesized poly(ethylene terephthalate-*co*-ethylene glycol-*co*-lactide) copolyesters via the melt reaction method. They showed excellent thermal stability, controllable degradation rates, high mechanical properties, and good biocompatibility. Furthermore, the copolyesters were found to exhibit reflection peaks similar to those of pristine poly(ethylene terephthalate) in wide-angle X-ray diffraction (WAXD) diffractograms. However, the synthetic process for the copolyesters was long and included the preparation of oligo lactic acid, a reaction *in vacuo*, and purification of the copolyesters. Furthermore, the processing of the copolyesters with a mold press was difficult and led to the formation of imperfect films. The relationship between the sequential structure and the crystallization of the copolyesters still needs further exploration. In this study, to develop an easier method for preparing the aromatic-aliphatic copolyesters by

direct melt transesterification and to investigate the cocrystallization behavior of these copolyesters, the thermoplastics PTT and PBS were reactively blended to afford poly(trimethylene terephthalate-*co*-butylene succinate) (PTTBS) copolyesters. The cocrystallization behavior of the resulting copolyesters induced by transesterification was studied to determine the relationship between the structure and properties of the copolyesters.

EXPERIMENTAL

Materials

PTT with a number-average molecular weight of 35,000 g/mol was purchased from Shell Chemical Co. (Texas, USA). PBS with a number-average molecular weight of 100,000 g/mol was purchased from Hexing Chemical Co. (Anhui, China). The solvents phenol and 1,1,2,2-tetrachloroethane were purchased from Tianjin Damao Chemical Reagent Factory (Tianjin, China) and were used directly as received.

Synthesis of the copolyesters

For reactive blending, PTT/PBS mixtures with different molar ratios (90/10, 80/20, 70/30, 60/40, 50/50, 40/60, 30/70, 20/80, and 10/90) were mixed in a 250-mL, three-necked glass flask equipped with a nitrogen inlet and outlet and a central mechanical stirrer. The reactor was slowly heated to 270°C under nitrogen protection and then stirred *in vacuo* for 2.5 h at the rate of 300 rpm. Then, the reaction mixture was cooled to room temperature and removed from the flask.

Nuclear magnetic resonance (NMR)

¹H-NMR spectra of the polyesters were obtained with a Bruker ARX 400 spectrometer (Ettlingen, Germany) operating at a frequency of 400 MHz for protons. Deuterated trifluoroacetic acid (DTFA) was used as the solvent, and tetramethylsilane ($\delta = 0$) was used as the internal standard.

Differential scanning calorimetry (DSC)

The melting and crystallization behaviors of the samples were determined on a Shimadzu DSC60 (Suzhou, China) calibrated with indium and zinc standards. The samples (ca. 5 mg) were annealed at 250°C for 3 min to erase the thermal history. Then, the samples were cooled to -50°C at a rate of 10°C/min and subsequently heated to 250°C at a rate of 10°C/min. The corresponding cooling and heating curves were then recorded. For the isothermal crystallization, the samples were quickly cooled to

different temperatures at a rate of 100°C/min and crystallized for 2 h after melting at 250°C for 3 min. Then, the samples were heated to 250°C at a rate of 10°C/min. The corresponding glass-transition temperature (T_g), crystallization temperature (T_c), melting temperature (T_m), crystallization enthalpy (ΔH_c), and melting enthalpy (ΔH_m) were recorded.

WAXD

The WAXD study of the samples was carried out on a Bruker D8 Focus X-ray diffractometer operated at 40 kV and 40 mA with a copper target (wavelength = 1.54 Å). The scanning angles (2θ) ranged from 3 to 40° with a step scanning rate of 2°/min. The samples were heated at temperatures 10°C above T_m (determined by DSC) for 3 min and cooled to temperatures 50°C below T_m to isothermally crystallize for 2 h.

Polarized optical microscopy (POM)

The samples, dissolved in a phenol/1,1,2,2-tetrachloroethane solution, were dropped onto a glass plate, and the solvent was evaporated at 80°C *in vacuo*. The specimens were then heated to different temperatures 10°C above T_m (determined by DSC) for 3 min, cooled rapidly to different temperatures 50°C below T_m at 100°C/min, and crystallized for 2 h. Then, the specimens were rapidly cooled to room temperature so that the morphology could be observed with a Nikon E600 POL polarized optical microscope (Tokyo, Japan) equipped with a camera.

Mechanical properties

The tensile strength, elongation at break, and Young's modulus were measured with a Sans CMT8502 machine (Shenzhen, China) according to GD203A at a crosshead speed of 20 mm/min. Measurements were carried out at room temperature. Thin films sandwiched between two polyamide films were prepared with a Kangsente MY-8200-10 hot press (Beijing, China). The samples were heated to the desired temperatures (10°C above T_m determined by DSC) for 3 min to erase the thermal history. Subsequently, the amorphous films were obtained via quenching in liquid nitrogen. The films were cut into sheets (22 mm × 5 mm) with a thickness of approximately 0.5 mm and used for the mechanical testing. At least five specimens were tested for each sample, and the average values are reported.

Hydrolysis degradation

The amorphous films (22 mm × 5 mm × 0.5 mm) used for mechanical testing were placed in a solu-

tion of NaOH (pH 10) to accelerate the degradation process. Each specimen was kept at $37 \pm 1^\circ\text{C}$ in an oven, and the medium was replaced every 3 days. At predetermined degradation time intervals, the specimens were removed from the medium, rinsed with distilled water, dried *in vacuo* at room temperature for 1 week, and weighed. The weight-loss percentages of the copolyesters were obtained according to the following relationship:

$$\text{Weight loss (\%)} = [(W_0 - W_r)/W_0] \times 100\% \quad (1)$$

where W_0 is the initial weight and W_r is the remaining weight of the specimen after degradation and drying.

RESULTS AND DISCUSSION

Structural analysis of the copolyesters

The PTTBS copolyesters were synthesized by direct melt transesterification of PTT and PBS with different molar ratios. After the mixture reacted at 270°C *in vacuo* for 2.5 h, it was taken out and used for further characterization. PTT is composed of terephthalate and propylene units, and PBS is composed of succinate and butylene units. Transesterification may eventually lead to the formation of terephthalate-propylene-terephthalate (TPT), terephthalate-butylene-terephthalate (TBT), terephthalate-propylene-succinate (TPS), terephthalate-butylene-succinate (TBS), succinate-propylene-succinate (SPS), and succinate-butylene-succinate (SBS) units. The protons in these units will probably exhibit different signals in $^1\text{H-NMR}$ spectra because of the different chemical environments.

Figure 1 shows the signals for protons of aromatic rings (a), protons of methylene groups of the succinic units (d), protons of methylene groups linked to the terephthalate (b), and protons of the middle methylene group (c). Additionally, some protons (e and f) are ascribed to the methylene groups linked to succinic units. Furthermore, there are several new signals between 4.0 and 5.0 ppm, and these confirm the formation of new units due to the transesterification between PTT and PBS. The assignment of the TPT, TBT, TPS, TBS, SPS, and SBS units is illustrated in Figure 1 and is based on previous studies.^{21,22} The fraction of each unit could be calculated on the basis of the integrated areas of the reflection signals according to the following equations:

$$f_{\text{TPT}} = \frac{A_{\text{TPT}}}{A}; f_{\text{TBT}} = \frac{A_{\text{TBT}}}{A}; f_{\text{TPS}} = \frac{A_{\text{TPS}}}{A};$$

$$f_{\text{TBS}} = \frac{A_{\text{TBS}}}{A}; f_{\text{SPS}} = \frac{A_{\text{SPS}}}{A}; f_{\text{SBS}} = \frac{A_{\text{SBS}}}{A} \quad (2)$$

$$A = A_{\text{TPT}} + A_{\text{TBT}} + A_{\text{TPS}} + A_{\text{TBS}} + A_{\text{SPS}} + A_{\text{SBS}} \quad (3)$$

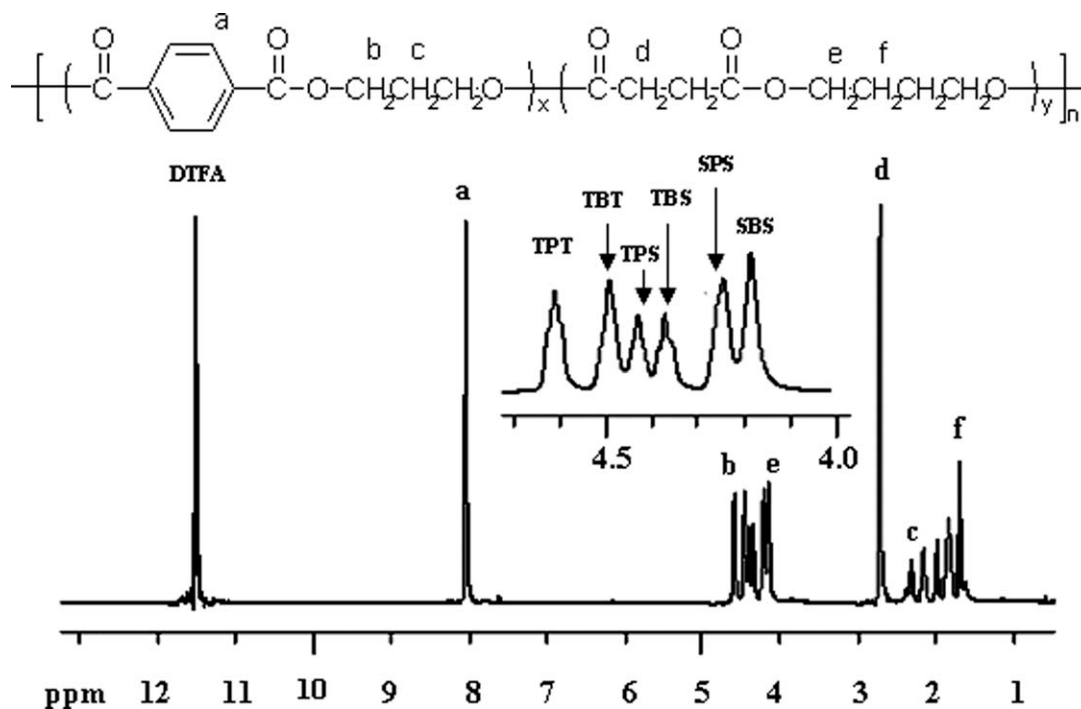


Figure 1 $^1\text{H-NMR}$ spectrum of the 50/50 PTTBS copolyester.

where A is the peak area of the signals calculated from the $^1\text{H-NMR}$ analysis and f represents the fraction of the area of each unit in the total area of the signals.

The molar fraction of aliphatic units ($P_{\text{PS}} + P_{\text{BS}}$) and the molar fraction of aromatic units (P_{TT}) could be calculated according to the following equations:

$$P_{\text{PS}} + P_{\text{BS}} = \frac{f_{\text{TPS}} + f_{\text{TBS}}}{2} + f_{\text{SPS}} + f_{\text{SBS}} \quad (4)$$

$$P_{\text{TT}} = \frac{f_{\text{TBS}} + f_{\text{TPS}}}{2} + f_{\text{TBT}} + f_{\text{TPT}} \quad (5)$$

The actual molar composition in all cases was quite close to the corresponding feed composition, as shown in Table I. The minor differences may have originated from the decomposition during the reaction process and the transesterification between PTT and PBS.

According to Yamadera and Murano,³⁴ the number-average sequence lengths for aromatic units (L_{nTT}) and aliphatic units ($L_{\text{nPS}} + L_{\text{nBS}}$) as well as the degree of randomness (R) could be obtained with the following equations:

$$L_{\text{nTT}} = \frac{2P_{\text{TT}}}{f_{\text{TBS}} + f_{\text{TPS}}} \quad (6)$$

$$L_{\text{nPS}} + L_{\text{nBS}} = \frac{2(P_{\text{PS}} + P_{\text{BS}})}{f_{\text{TBS}} + f_{\text{TPS}}} \quad (7)$$

$$R = \frac{1}{L_{\text{nTT}}} + \frac{1}{L_{\text{nBS}} + L_{\text{nPS}}} \quad (8)$$

The results for L_{nTT} and $L_{\text{nPS}} + L_{\text{nBS}}$ are illustrated in Table I. As the PBS content increased, the aromatic sequence length decreased, and the aliphatic sequence length increased.

It is generally accepted that upon the blending of two condensation homopolymers, the occurrence of transesterification leads to the formation of block copolymers, with the block length gradually decreasing during the blending process.^{10,11} In the case of random copolymers, R takes a value equal to 1,

TABLE I
BS Contents of the Copolyesters, R Values, and L_{nTT}
and $L_{\text{nPS}} + L_{\text{nBS}}$ Values

PTT/ PBS	BS (mol %)		L_{nTT}^a	$L_{\text{nPS}} + L_{\text{nBS}}^a$	R
	Feed composition	Composition by $^1\text{H-NMR}$			
90/10	10	9.0	10.72	1.41	0.81
80/20	20	20.0	6.25	1.72	0.74
70/30	30	28.8	3.34	2.23	0.75
60/40	40	42.6	2.56	2.59	0.83
50/50	50	51.0	2.11	2.90	0.83
40/60	60	56.4	1.89	3.55	0.80
30/70	70	62.1	1.77	3.65	0.84
20/80	80	74.8	1.50	5.62	0.84
10/90	90	90.2	1.26	8.00	0.92

^a Calculated from $^1\text{H-NMR}$ spectra.

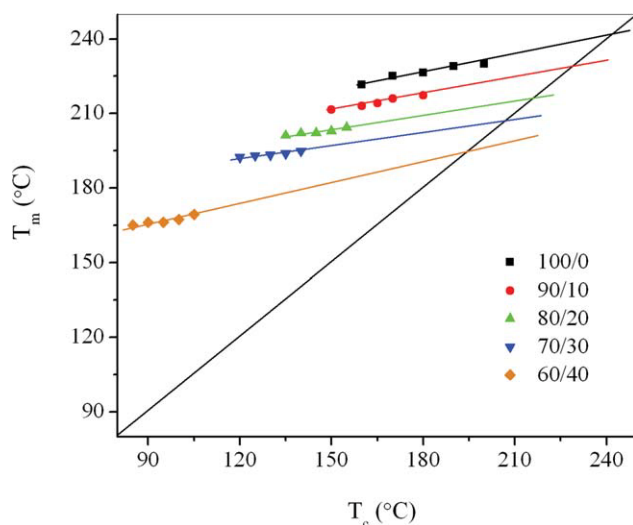


Figure 2 Hoffman–Weeks plots for the determination of the T_m^0 values of PTT and its copolyesters. [Color figure can be viewed in the online issue, which is available at wileyonlinelibrary.com.]

whereas for alternating copolymers, R is equal to 2, and for block copolymers, it is close to 0. In all cases, as illustrated in Table I, R was equal to 0.8 after 2.5 h of reaction, and this showed that the copolyesters were almost random.

Melting point depression

The equilibrium melting temperature (T_m^0) is defined as the melting temperature of lamellar crystals with an infinite thickness. The Hoffman–Weeks method was used to estimate T_m^0 of the copolyesters with BS contents less than 40%, and the corresponding results are illustrated in Figure 2. T_m^0 of the copolyesters decreased as the BS unit content increased, and this showed that the incorporation of BS segments interrupted the crystallization of the lamellae. The lamellae of the copolyesters containing more BS units were supposed to be thinner because of the lower T_m values.

The melting point depression of the PTTBS copolyesters was further analyzed with the Flory,²⁹ Sanchez–Eby,³⁰ and Baur³¹ equations and the Wending–Suter model³² for the cocrystallization of copolymers of TT and BS comonomers, and the results are shown in Figure 3.

In the case of comonomer exclusion, the Flory equation can be presented as follows:

$$\frac{1}{T_m^0} - \frac{1}{T_m(X_B)} = \frac{R}{\Delta H_m^0} \ln(1 - X_B) \quad (9)$$

where X_B is the concentration of minor BS units in the polymer and $\ln(1 - X_B)$ equals the collective activities of TT sequences in the limit of the upper

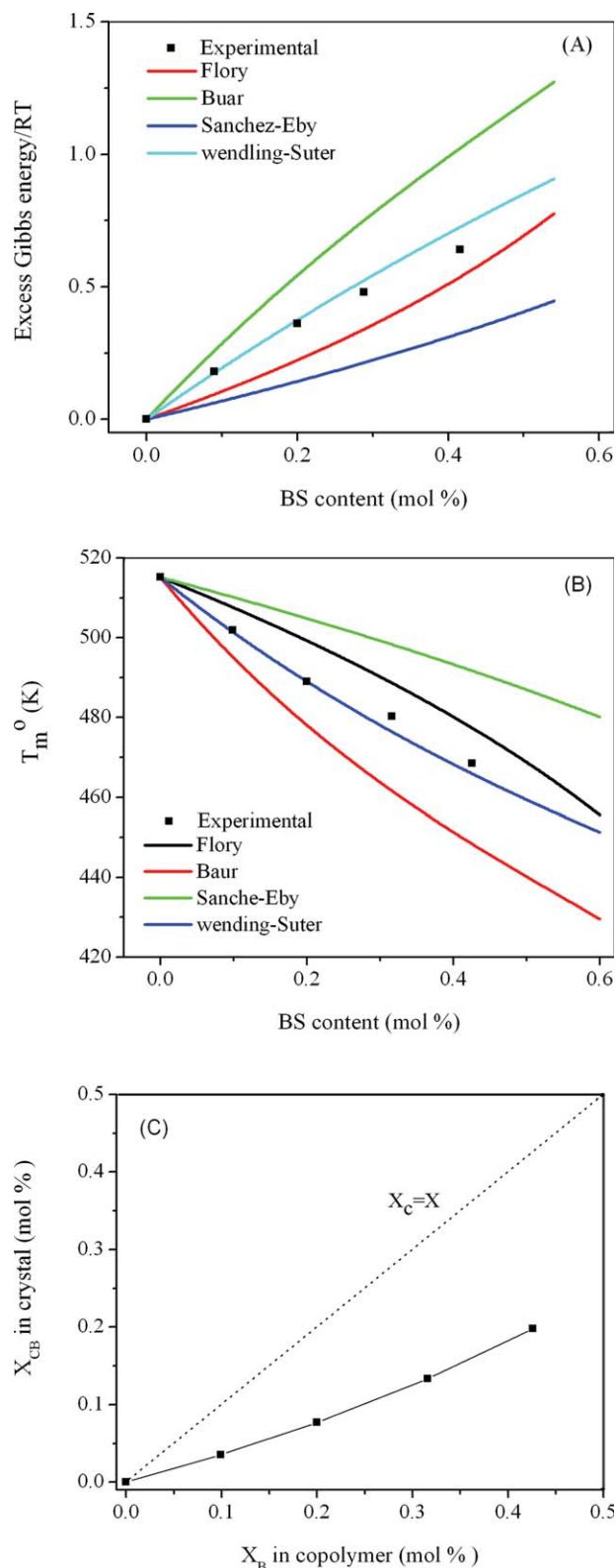


Figure 3 (A) Excess Gibbs energy/ RT from experimentation and from the Flory, Baur, Sanchez–Eby, and Wending–Suter models, (B) comparison of the theoretical T_m^0 values and experimental values, and (C) equilibrium concentrations of BS units incorporated into the PTT crystal as a function of the copolyester composition. [Color figure can be viewed in the online issue, which is available at wileyonlinelibrary.com.]

bound of T_m . T_m^0 and ΔH_m^0 represent the homopolymer PTT equilibrium melting temperature and heat of fusion, respectively, and R is the gas constant.

According to the Sanchez–Eby model, the BS units can be included in the crystals of TT, in which they act as defects. The model is defined as the inclusion model, and the equation is

$$\frac{1}{T_m^0} - \frac{1}{T_m(X_B)} = \frac{R}{\Delta H_m^0} \ln(1 - X_B + X_B e^{-\varepsilon/RT}) \quad (10)$$

where $X_B e^{-\varepsilon/RT}$ is the equilibrium fraction of BS units, T is the temperature, and ε is the excess free energy of a defect created by the incorporation of one BS unit into the crystal.

Baur³¹ suggested that the copolyester crystals could be treated as a pseudo-eutectic system, and the equation can be presented as follows:

$$\frac{1}{T_m^0} - \frac{1}{T_m(X_B)} = \frac{R}{\Delta H_m^0} \left[\ln(1 - X_B) - \langle \xi \rangle^{-1} \right] \quad (11)$$

where $\langle \xi \rangle = [2X_B(1 - X_B)]^{-1}$ is the average length of the homopolymer sequence in the melt. The homopolymer sequences of length ξ may be included in crystals with a lamellar thickness corresponding to that length.

Apart from these models, the Wendling–Suter equation, combining both the exclusion and inclusion models, could also be applied to depict the melting point depression of the copolyesters:

$$\frac{1}{T_m^0} - \frac{1}{T_m(X_B)} = \frac{R}{\Delta H_m^0} \left[\frac{\varepsilon X_{CB}}{RT} + (1 - X_{CB}) \times \ln \frac{1 - X_{CB}}{1 - X_B} + X_{CB} \ln \frac{X_{CB}}{X_B} - \langle \xi \rangle^{-1} \right] \quad (12)$$

where X_{CB} is the concentration of BS units in the crystal. $\langle \xi \rangle$ is determined as follows:

$$\langle \xi \rangle^{-1} = 2(X_B - X_B e^{-\varepsilon/RT})(1 - X_B + X_B e^{-\varepsilon/RT})$$

If the comonomers are completely included in the crystals, the concentration of BS units will be calculated with the following equation:

$$X_{CB}^{\text{eq}} = \frac{X_B e^{-\varepsilon/RT}}{1 - X_B + X_B e^{-\varepsilon/RT}} \quad (13)$$

where X_{CB}^{eq} is equilibrium concentration of BS units incorporated into the PTT crystal.

In Figure 3(A), the experimental excess crystallization Gibbs energy $\{[\Delta H_m^0/(RT_m)] \times (1 - T_m/T_m^0)\}$ is plotted together with the theoretical values calculated as a function of the copolyester composition. For the Flory, Baur, Sanchez, and Wendling–Suter models, the excess free energy is calculated as

$\ln(1 - X_B)$, $\ln(1 - X_B) - \langle \xi \rangle^{-1}$, $\ln(1 - X_B + X_B e^{-\varepsilon/RT})$, and $X_{CB}/RT + (1 - X_{CB})\ln(1 - X_{CB})/(1 - X_B) + X_{CB} \ln(X_{CB}/X_B) - \langle \xi \rangle^{-1}$, respectively. The Wendling–Suter model fit the experiment better than the other models, and this showed that the comonomer BS units were incorporated into the TT crystals by the exclusion and inclusion methods. Additionally, the Flory model also seemed to be able to predict the excess free energy of the copolyesters. In Figure 3(B), the T_m^0 values calculated with the Flory, Baur, Sanchez, and Wendling–Suter models are shown in comparison with the experimental values. The Wendling–Suter model was more realistic and provided values lower than the experimental data. This indicated that the inclusion and exclusion of the comonomers in the homopolymer crystals existed in the cocrystallization of the copolyesters.

To further estimate the percentage of BS units incorporated into the crystals, the results from the Wendling–Suter model were further analyzed according to eq. (13). The plot of the equilibrium concentration of BS units in the PTT crystal (X_{CB}) versus the concentration of BS units in the copolyesters (X_B) is shown in Figure 3(C). It is revealed that X_{CB} increased as X_B increased. Although X_{CB} was not low, it was lower than X_B .

Crystallization and melting behaviors of the copolyesters

The results for the melting point depression indicated the cocrystallization of the copolyesters. Therefore, the crystallization and melting behaviors of the copolyesters were further analyzed with DSC, as shown in Figure 4; the corresponding data are illustrated in Table II. T_c and T_m of the polymer first decreased and then increased as the BS unit content increased. The 40/60 and 30/70 copolyesters showed no crystallization or melting peaks because of the short sequence lengths of both the TT and BS units, as shown in Table I. Magnifying the DSC curves, we found only one T_g in Figure 4, and this indicated that no phase separation occurred in the copolyesters. The 50/50, 40/60, 30/70, 20/80, and 10/90 copolyesters showed one clear T_g ; however, the other copolyesters showed an obscure glass transition during the heating process. It is known that the glass transition is dependent on the degree of the amorphous region in semicrystalline polymers. A high degree of crystallinity after cooling from the melting state probably leads to no obvious T_g values.

Except for the 40/60 and 30/70 copolyesters, the other copolyesters exhibited almost only one crystallization and melting peak during the cooling and heating process. This supports the idea that the copolyesters exhibited cocrystallization behavior because of the compatibility of the TT and BS units in their

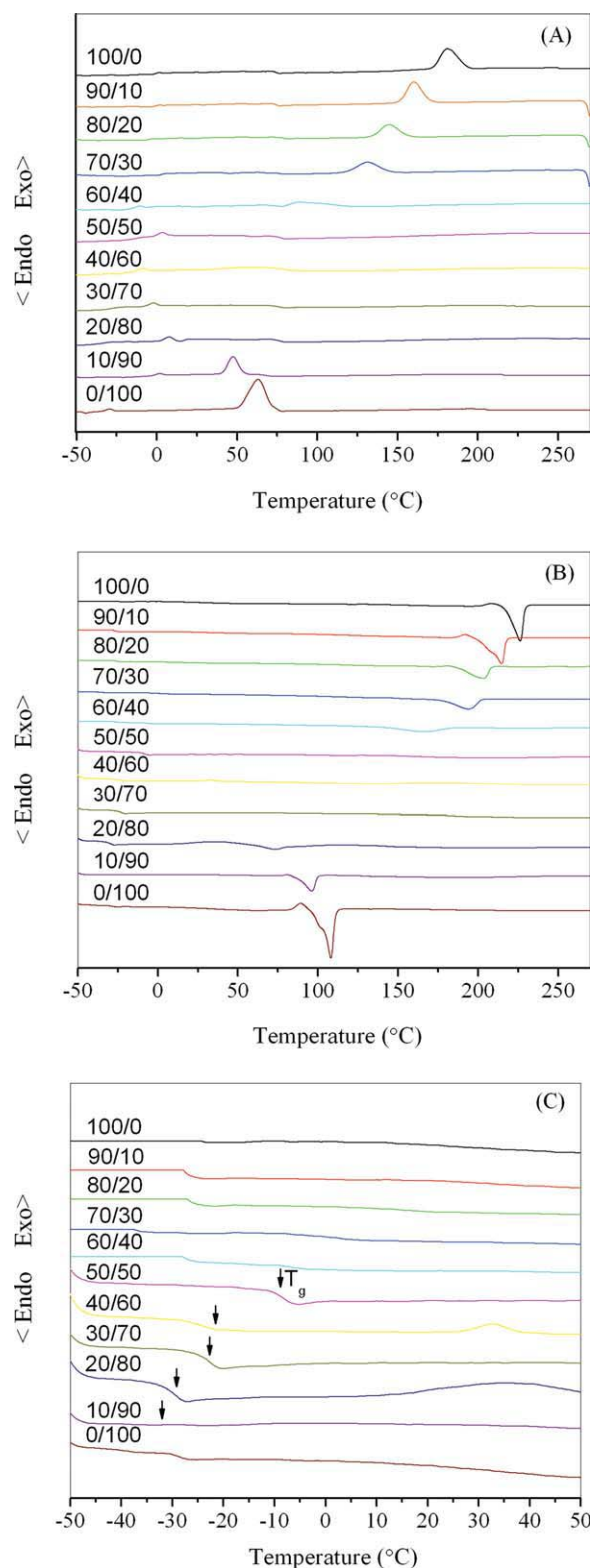


Figure 4 (A) DSC cooling curves, (B) DSC heating curves, and (C) expanded DSC heating curves for copolyesters with different compositions. [Color figure can be viewed in the online issue, which is available at wileyonlinelibrary.com.]

crystal lattices. When the T_m values of the copolyesters were compared as a function of the actual copolyester composition determined by $^1\text{H-NMR}$ analysis,

TABLE II
DSC Data for the PTTBS Copolyesters

PTT/ PBS	T_m ($^{\circ}\text{C}$)	T_c ($^{\circ}\text{C}$)	T_g ($^{\circ}\text{C}$)	ΔH_m (J/g)	ΔH_c (J/g)
100/0	226.2	181.1	46.5	58.4	50.3
90/10	214.6	160.2	26.3	52.4	42.4
80/20	203.0	144.8	15.1	31.3	32.8
70/30	193.8	131.4	8.8	27.5	31.0
60/40	166.2	88.7	-3.3	20.6	15.9
50/50	136.7	— ^a	-14.2	0.4	—
40/60	117.3	—	-20.6	—	—
30/70	—	—	-21.8	—	—
20/80	73.2	37.9	-27.0	24.6	5.2
10/90	96.2	47.4	-27.8	44.9	48.5
0/100	108.0	63.2	-32.3	78.0	67.6

^a The data could not be determined by DSC analysis.

as illustrated in Figure 5, a minimum T_m value was observed at the BS unit content of approximately 70% via the fitting of the curves of the obtained T_m values according to the Wendling–Suter equation. This indicated that the crystal structure transition of the copolyesters might appear at the BS unit content of 70%. Cocrystallization is generally classified into two types: isomorphism and isodimorphism. This depends on the existence of a eutectic point at which the crystalline structures change from one type to the other type.²⁸ Consequently, the PTTBS copolyesters exhibited isodimorphic cocrystallization according to the aforementioned results.

WAXD analysis and cocrystallization behavior

Figure 6 shows the X-ray spectra of the copolyesters isothermally crystallized at temperatures 50 $^{\circ}\text{C}$ below the T_m values of the copolyesters, and the

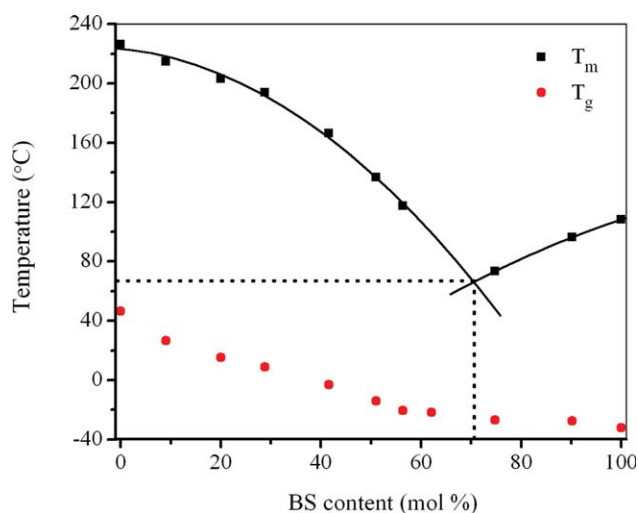


Figure 5 T_m and T_g for the PTTBS copolyesters. The Kwei prediction for the T_g values of the copolyesters is also plotted. [Color figure can be viewed in the online issue, which is available at wileyonlinelibrary.com.]

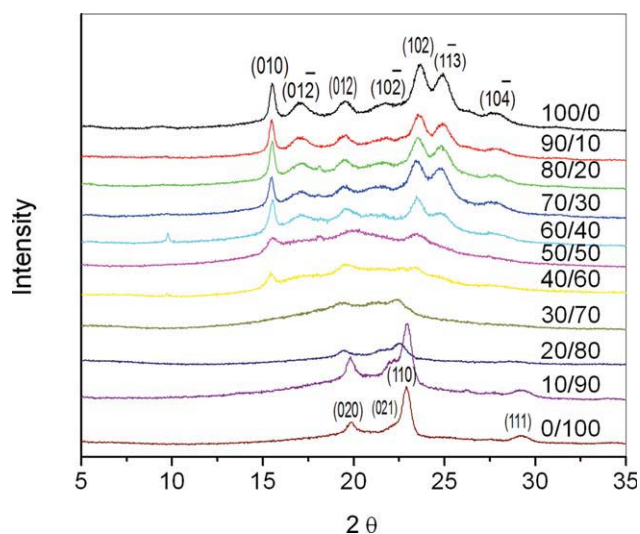


Figure 6 WAXD patterns of the PTTBS copolyesters. [Color figure can be viewed in the online issue, which is available at wileyonlinelibrary.com.]

corresponding Miller index is also presented. All the copolyesters exhibited clear diffraction peaks, and the diffraction peaks of the 50/50, 40/60, and 30/70 copolyesters were weaker than those of the other copolyesters. For the copolyesters with BS unit contents less than 60%, the copolyesters showed reflection peaks similar to those of PTT, and this indicated that the copolyesters formed a triclinic crystal structure. In addition, the positions of the reflection peaks showed no significant change in comparison with those of pristine PTT. For the copolyesters with BS unit contents greater than 70%, the copolyesters exhibited reflection peaks similar to those of PBS, and this showed that the copolyesters formed crystal structures similar to that of PBS. We further noticed that the position of the reflection peaks slightly shifted to higher angles as the BS unit content increased. The crystal structure seemed to change at the BS unit molar fraction of 70%, and this was consistent with the analysis of the T_m values of the copolyesters by DSC.

In copolyesters such as poly(butylene-*co*-propylene succinate) and poly(propylene terephthalate-*co*-succinate), the positions of the reflection peaks change almost linearly as the content of the second component increases.^{21,22,24–28} The aforementioned results are different from those of previous studies of the cocrystallization behavior of copolyesters. First, the positions of the diffraction peaks remained unchanged at BS unit contents below 60%. Second, the positions of the diffraction peaks for the copolyesters changed slightly when the BS unit contents were greater than 70%, and this showed that the TT units might have been incorporated into the crystal structure of PBS. Therefore, it could be concluded that the copolyesters exhibited isodimorphic cocrystallization behaviors according to the X-ray spectra.

Spherulitic morphology

The spherulitic morphologies of the PTTBS copolyesters are shown in Figure 7. The samples were isothermally crystallized at temperatures 50°C below the T_m values. However, the 40/60 and 30/70 PTTBS copolyesters showed no spherulites or crystals according to POM, and this showed that it was difficult for these copolyesters to form spherulites with large scales because of the randomness of the molecular chains; this was consistent with the results of the DSC analysis.

As shown in Figure 7(a), the pristine PTT exhibited ring-banded spherulites similar to the results reported in the literature.^{16,17} The 90/10 copolyester exhibited light yellow spherulites with clear boundaries between the spherulites. The 80/20 and 70/30 copolyesters showed ring-banded spherulites, whereas the 60/40 copolyester showed spherulites much smaller in diameter. For the 50/50 copolyester, no significant spherulites were observed except for some bright dots, and this indicated that the copolyester was difficult to crystallize under these conditions. For the 20/80 copolyester, the spherulites that were dispersed in the POM graphs were not fully grown. For the 10/90 copolyester, the spherulites showed clear boundaries similar to those of pristine PBS. On the basis of these results, the spherulitic diameters of the copolyesters first decreased and then increased with the PBS content increasing at the same undercooling. This phenomenon was similar to the change in T_m with the BS content, which was originally determined by the aromatic and aliphatic sequence length. The sequential structure significantly affected the crystallization behaviors of the copolyesters, which eventually influenced the morphology of the copolyester spherulites.

Mechanical properties

Tensile properties, such as the tensile strength, elongation at break, and elastic modulus, were determined for samples prepared from the melt and quenched in liquid nitrogen. The results are illustrated in Table III. The tensile strength as well as the elastic modulus decreased and then increased as the BS unit content increased. Furthermore, the 70/30 and 60/40 copolyesters exhibited much higher elongation at break than the pristine PTT. The 20/80 and 10/90 copolyesters also exhibited higher elongation at break than PBS. The 50/50, 40/60, and 30/70 copolyesters showed weak mechanical properties.

On the basis of the ¹H-NMR analysis, the 50/50, 40/60, and 30/70 copolyesters had shorter aromatic sequence lengths and longer aliphatic sequence lengths in comparison with the 70/30 and 60/40 copolyesters. In addition, they had shorter aliphatic sequence lengths than the 20/80 and 10/90

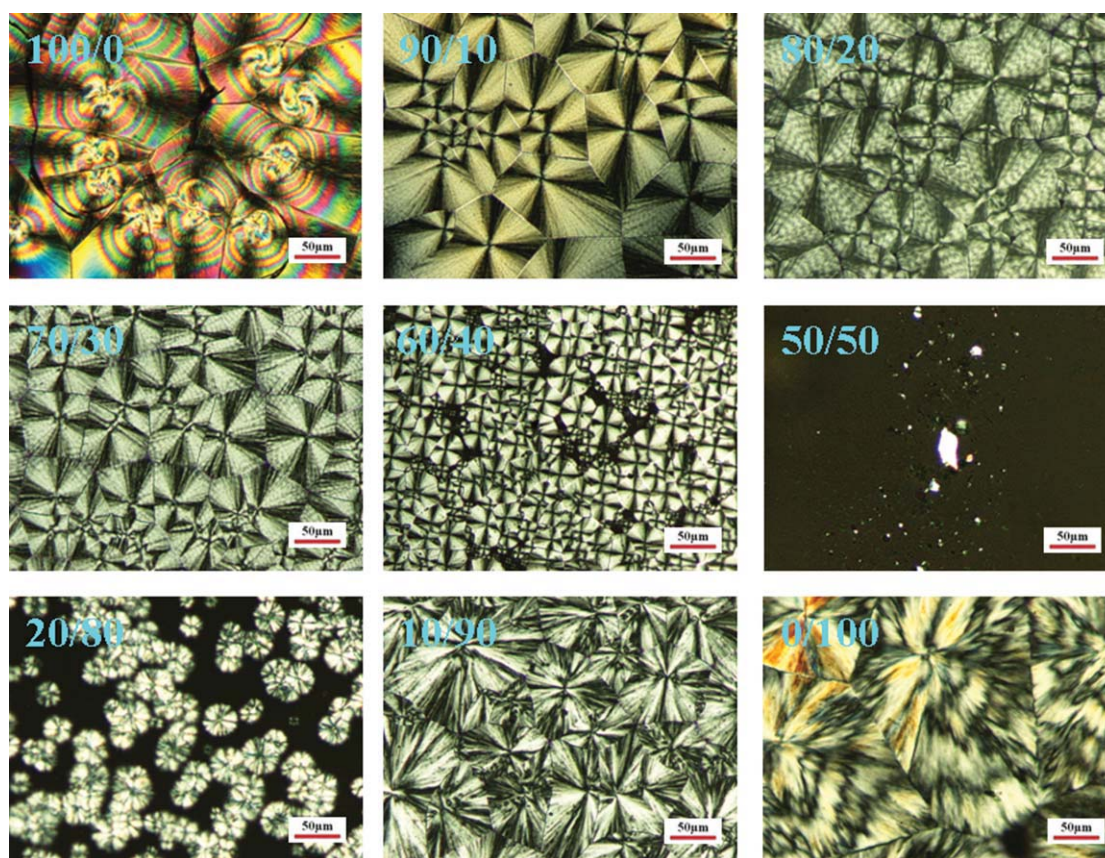


Figure 7 POM images of the PTTBS copolyesters isothermally crystallized at temperatures 50°C below their T_m values. [Color figure can be viewed in the online issue, which is available at wileyonlinelibrary.com.]

copolyesters. The appropriate sequence length of the aromatic and aliphatic units was supposed to determine the mechanical properties of the copolyesters. The longer aromatic and aliphatic sequence lengths facilitated the improvement of the mechanical properties of the copolyesters. However, too long or too short sequence lengths of both the aromatic and aliphatic units might have degraded the mechanical properties of the copolyesters. It is suggested that the sequential structure of the copolyesters determined the mechanical properties of the copolyesters. It is generally accepted that the mechanical properties of polymers are also dependent on their aggregation structure. On the basis of the DSC, WAXD, and POM results, the copolyesters showed different crystallization and melting behaviors. The crystal structure and spherulitic morphology of the copolyesters were also influenced by the BS unit content. Factors such as the degree of crystallinity, the diameter of the spherulites, and the crystal form greatly affected the mechanical properties of the copolyesters. The higher degree of crystallinity and the PTT crystal structure facilitated the improvement of the tensile strength and elastic modulus. The spherulites, relatively large in diameter, made the copolyesters brittle because of the weak interactions between the

interfaces of the spherulites. However, because of the differences in the chemical structures of the copolyesters, the relationship between the aggregation structure and the mechanical properties of the copolyesters was somewhat complex.

Hydrolytic degradation

It is well known that the hydrolytic degradation rates of polyesters depend on many factors, such as

TABLE III
Mechanical Properties of the Copolyesters

PTT/ PBS	Tensile strength (MPa)	Elongation at break (%)	Elastic modulus (MPa)
100/0	49.9 ± 2.2	350 ± 20	1774 ± 190
90/10	42.0 ± 1.8	310 ± 30	2041 ± 210
80/20	38.3 ± 2.2	432 ± 40	956 ± 112
70/30	24.5 ± 2.4	661 ± 45	120 ± 21
60/40	38.1 ± 3.2	527 ± 40	318 ± 32
50/50	1.9 ± 1.8	264 ± 60	24 ± 16
40/60	8.8 ± 1.2	392 ± 30	20 ± 12
30/70	1.7 ± 1.4	172 ± 55	10 ± 8
20/80	17.6 ± 2.1	450 ± 40	142 ± 18
10/90	26.2 ± 2.3	626 ± 50	419 ± 52
0/100	32.6 ± 2.4	100 ± 20	722 ± 48

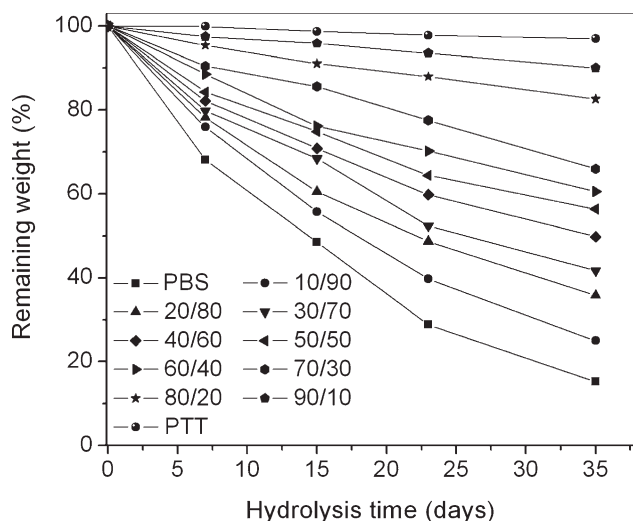


Figure 8 Remaining weight versus the time of hydrolysis for the PTTBS copolyesters.

the chemical structure, the degree of crystallinity, the crystal form, and the molecular mobility of the amorphous phase. Figure 8 shows the degradation behavior of the PTTBS copolyester films prepared from the melt and quenched in liquid nitrogen. As expected, the degradation rate of the copolyesters increased as the BS unit content increased. This indicated that the relatively short aromatic sequence length and long aliphatic sequence length facilitated hydrolysis in a solution of NaOH.

CONCLUSIONS

Copolyesters based on PTT and PBS were successfully prepared by direct melt transesterification. The $^1\text{H-NMR}$ results indicated that the copolyesters were almost random with a composition similar to the feed molar ratio. The aromatic sequence length decreased, whereas the aliphatic sequence length increased, as the BS unit content increased. The melting point depression predicted by the models indicated that the Wendling–Suter and Flory models could be used to describe the cocrystallization behavior of the copolyesters. Both DSC and WAXD results showed that the copolyesters exhibited isomorphous cocrystallization, and the transformation for both T_m and the crystal form happened at a BS content of approximately 70%. The sequence lengths of aromatic and aliphatic units influenced the morphology of the spherulites, mechanical properties, and hydrolytic degradation of the copolyesters. The relatively long aromatic and aliphatic sequence lengths of the copolyesters indicated strong mechanical properties. The relatively short aromatic sequence length and long aliphatic sequence length of the copolyesters facilitated hydrolysis in a solution of NaOH. This article demonstrates an easy method for

the preparation of degradable aromatic–aliphatic copolyesters that can be applied to other systems. The cocrystallization phenomenon will exist in almost all copolyesters composed of crystallizable components. An investigation of cocrystallization may help us to design copolyesters with desired crystal forms, T_m values, and mechanical and degradation properties.

References

- Nair, L. S.; Laurencin, C. T. *Prog Polym Sci* 2007, 32, 762.
- Li, F.; Xu, X.; Hao, Q.; Li, Q.; Yu, J.; Cao, A. *J Polym Sci Part B: Polym Phys* 2006, 44, 1635.
- Nagata, M.; Goto, H.; Sakai, W.; Tsutsumi, N. *Polymer* 2000, 41, 4373.
- González, V. N.; De Ilarduya, A. M.; Herrera, V.; Muñoz-Guerra, S. *Macromolecules* 2008, 41, 4136.
- Li, W. D.; Zeng, J. B.; Li, Y. D.; Wang, Y. Z. *J Polym Sci Part A: Polym Chem* 2009, 47, 5898.
- Szymczyk, A. *Eur Polym J* 2009, 45, 2653.
- Kondratowicz, F.; Ukielski, R. *Polym Degrad Stab* 2009, 94, 375.
- Pisula, W.; Pigłowski, J.; Kummerlöwe, C. *Polimery* 2006, 51, 341.
- Jeong, Y. G.; Jo, W. H. *Macromolecules* 2003, 36, 4051.
- Salhi, S.; Tessier, M.; Blais, J. C.; Gharbi, R. E.; Fradet, A. *Macromol Chem Phys* 2004, 205, 2391.
- Wang, L. C.; Xie, Z. G.; Bi, X. J.; Wang, X.; Zhang, A. Y.; Chen, Z. Q.; Zhou, J. Y.; Feng, Z. G. *Polym Degrad Stab* 2006, 91, 2220.
- Kint, D. P. R.; Alla, A.; Deloret, E.; Campos, J. L.; Guerra, S. M. *Polymer* 2003, 44, 1321.
- Shi, X. Q.; Aimi, K.; Ito, H.; Ando, S.; Kikutani, T. *Polymer* 2005, 46, 751.
- Shi, X. Q.; Ito, H.; Kikutani, T. *Polymer* 2005, 46, 11442.
- Acar, I.; Pozan, G. S.; Özgümüş, S. *J Appl Polym Sci* 2008, 109, 2747.
- Desborough, I. J.; Hall, I. H.; Neisser, J. Z. *Polymer* 1979, 20, 545.
- Lorenzetti, C.; Finelli, L.; Lotti, N.; Vannini, M.; Gazzanoc, M.; Berti, C.; Munari, A. *Polymer* 2005, 46, 4041.
- Karayannidis, G. P.; Roupakias, C. P.; Bikiaris, D. N.; Achilias, D. S. *Polymer* 2003, 44, 931.
- Papageorgiou, G. Z.; Bikiaris, D. N. *Polymer* 2005, 46, 12081.
- Rizzarelli, P.; Carroccio, S. *Polym Degrad Stab* 2009, 94, 1825.
- Papageorgiou, G. Z.; Bikiaris, D. N. *Biomacromolecules* 2007, 8, 2437.
- Papageorgiou, G. Z.; Vassiliou, A. A.; Karavelidis, V. D.; Koumbis, A.; Bikiaris, D. N. *Macromolecules* 2008, 41, 1675.
- Rizzarelli, P.; Puglisi, C.; Montaudo, G. *Polym Degrad Stab* 2004, 85, 855.
- Lee, J. H.; Jeong, Y. G.; Lee, S. C.; Min, B. G.; Jo, W. H. *Polymer* 2002, 43, 5263.
- Pan, P. J.; Inoue, Y. *Prog Polym Sci* 2009, 34, 605.
- Mazzocchetti, L.; Scandola, M. *Macromolecules* 2009, 42, 7811.
- Cranston, E.; Kawada, J.; Raymond, S.; Morin, F. G.; Marchessault, R. H. *Biomacromolecules* 2003, 4, 995.
- Jeong, Y. G.; Lee, J. H.; Lee, S. C. *Polymer* 2009, 50, 1559.
- Flory, P. J. *J Chem Phys* 1947, 15, 684.
- Sanchez, I. C.; Eby, R. K. *Macromolecules* 1975, 8, 638.
- Baur, V. H. *Macromol Chem* 1966, 98, 297.
- Wendling, J.; Gusev, A. A.; Suter, U. W. *Macromolecules* 1998, 31, 2509.
- Tan, L. C.; Chen, Y. W.; Zhou, W. H.; Li, F.; Chen, L.; He, X. H. *Polym Eng Sci* 2010, 50, 76.
- Yamadera, M.; Murano, N. *J Polym Sci* 1967, 5, 2259.